

Deformation and yield of epoxy networks in constrained states of stress

R. S. KODY, A. J. LESSER*

Polymer Science and Engineering Department, University of Massachusetts, Amherst, MA 01003, USA

A series of epoxy networks were made with molecular weights between crosslinks, M_c , ranging from 380 to 1790 g mol⁻¹. Resins were cast into thin walled hollow cylinders and tested in stress states ranging from uniaxial compression to biaxial tension. These tests elucidated the effects of stress state, strain rate, and M_c on the yield and fracture response of epoxy networks. Throughout the study, the strain rate along the octahedral shear plane, $\dot{\gamma}^{\text{oct}}$, was maintained constant independent of stress state, for each failure envelope. The hollow cylinder tests showed that the yield behaviour of epoxy networks can be described by a modified von Mises criterion, $\tau_y^{\text{oct}} = \tau_{y0}^{\text{oct}} - \mu\sigma_m$ where τ_g^{oct} is the octahedral shear stress at yield, τ_{y0}^{oct} is the octahedral shear stress at yield in pure shear, μ is the coefficient of internal friction and V_m is the hydrostatic tensile stress imposed on the sample. Furthermore, these tests showed that changes in $\dot{\gamma}^{\text{oct}}$ and M_c only affect τ_{y0}^{oct} , while μ remains constant. Standard tensile and compression tests were run to confirm the hollow cylinder result and to test the effect of temperature on the yield and brittle response. Tensile tests showed that changes in M_c only affect the glass transition temperature, T_g , of the materials, and the glassy modulus remained independent of M_c . With regard to the yield strength, changes in M_c cause a shift in the T_g of the materials, and the yield strengths of all the materials collapse together at a constant temperature relative to T_g . Finally, yielding of these epoxies was shown to follow an Eyring type flow model over the range of temperatures and strain rates tested.

1. Introduction

Epoxy resins are extensively used in a variety of applications that subject them to multiaxial states of stress. In composite and adhesive applications, these stresses arise from the constraints imposed by the reinforcement or substrate in combination with the loading conditions. Yet surprisingly little is known about how these materials yield and fracture when subjected to these stress states.

Every relevant study to date has demonstrated that the yield and fracture responses of polymeric materials are sensitive to hydrostatic pressure. Early studies have shown that the yield behaviour of many glassy polymers can be described by a modified von Mises criterion [1–5].

$$\tau_y^{\text{oct}} = \tau_{y0}^{\text{oct}} - \mu\sigma_m \quad (1)$$

where τ_y^{oct} is the octahedral shear stress at yield, τ_{y0}^{oct} is the octahedral shear stress at yield in pure shear, μ is the coefficient of internal friction, and σ_m is the hydrostatic tensile stress imposed on the sample. However, none of these studies have shown how τ_{y0}^{oct} and μ are affected by changes in strain rate, temperature and molecular architecture. With regard to epoxies,

Sultan and McGarry [2] showed that Equation 1 generally describes the yield response of epoxy networks. For the case of a diglycidal ether of bis-phenol A (DGEBA) cured with Shell Corporation's curing agent D, they obtained values of $\tau_{y0}^{\text{oct}} = 39$ MPa and $\mu = 0.175$. Again, no mention of the effects of strain rate, temperature or molecular architecture on τ_{y0}^{oct} and μ was made. In 1980, Kinloch [6] summarized the reported values of τ_{y0}^{oct} and μ for several different polymers and stated that, in general, τ_{y0}^{oct} and μ would be affected by changes in strain rate and temperature, but presented no data to suggest how these parameters might change.

There have been several studies on the effects that σ_m has on the yield behaviour of glassy polymers [1–5, 7–11]. Some authors even tested the effect of strain rate on τ_{y0}^{oct} and μ , but multiple sample geometries were used to arrive at the different stress states [4, 5, 12, 13]. This approach severely limits the number of different stress states that can be investigated and convolutes the results with effects of fabricating different specimen geometries. In studies where single geometries were used [1–4, 7–9], the viscoelastic response of the materials was not fully considered. In the work

*Author to whom correspondence should be addressed.

we present here, attention is given to ensure that the strain rate along the octahedral shear plane, $\dot{\gamma}^{\text{oct}}$, is maintained constant for all stress states investigated.

Another goal of this work was to investigate the relationship between molecular architecture and material properties. Epoxy networks are ideal for this purpose due to the accuracy with which the molecular weight between crosslinks, M_c , can be controlled. There have been several studies on the effect that changing M_c has on the mechanical properties of epoxies [14, 15], but none considered a generalized stress state. Moreover, commercial resins and curing agents were often used in these tests, limiting the available specifics of molecular architecture. Often the crosslinking agents and chain extenders used had significantly different structures, which convoluted the effects of changing M_c . To date, no study has investigated how the generalized yield and fracture behaviour of glassy polymers is affected by intrinsic material characteristics (e.g. M_c ; glass transition temperature, T_g ; chain stiffness; etc.). Hence a complete understanding of how the yield and fracture behaviour of glassy polymers is affected by stress state, strain rate, temperature and M_c is not currently available.

This paper presents the results of an experimental investigation whose aim was to elucidate the yield and fracture response of epoxy networks and relate this response to the state of stress, strain rate, testing temperature and M_c . We chose a specimen geometry and test configuration that allows us to continuously vary the state of stress from uniaxial compression to biaxial tension. Moreover, our test strategy of keeping $\dot{\gamma}^{\text{oct}}$ constant over all stress states, allows us to consistently interrogate the strain rate effects while changing the state of stress. We also conducted these tests on model resin and curing agent systems, which pro-

vided us accurate control of M_c [16]. In a subsequent paper [17], we will propose a phenomenological model that accounts for changes in yield strength, due to changes in stress state, strain rate, testing temperature and M_c .

2. Experimental

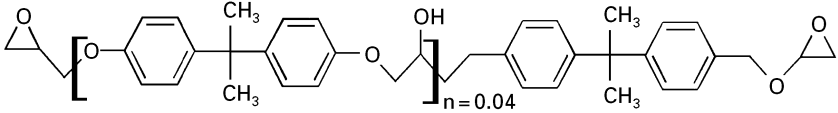
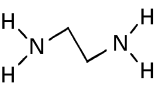
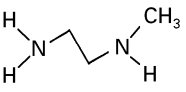
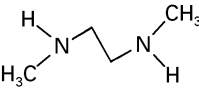
2.1. Materials

The materials were chosen to provide accurate control of the molecular architecture. The structure and properties of the resin and curing agents used are shown in Table I. Rather than use a commonly used commercial resin, the DGEBA was chosen for its narrow molecular weight distribution, $M_w/M_n = 1.01$. Ethylenediamine (EDA), methylethylenediamine (MEDA) and N,N-dimethylethylenediamine (DMEDA) were chosen as the curing agents for their low molecular weights and similar structures. The DMEDA and MEDA were purchased as a mixture of 85 wt % DMEDA and 15 wt % MEDA. The EDA and MEDA behave as crosslinking agents, while DMEDA is a chain extender. The low molecular weights of the curing agents allow the properties of the network to be dictated primarily by the resin. The similarity of the curing agents' structures assures that the polymer backbone stiffness is not significantly altered by changing M_c .

The resin and curing agents were mixed stoichiometrically. By varying the amounts of EDA and MEDA/DMEDA, samples were prepared with five different molecular weights between crosslinks, $M_c = 380, 480, 640, 950$ and 1790 g mol^{-1} . Calculations for M_c were made using the following equation:

$$M_c = \frac{2(M_e + \sum_{f=2}^{\infty} (M_f/f) \Phi_f)}{\sum_{f=3}^{\infty} (\Phi_f)} \quad (2)$$

TABLE 1 Chemical structures and properties of the resin and curing agents

Chemical name Structure	Functionality y	M_w (g mol^{-1})
Diglycidyl ether of Bis-phenol A (DGEBA) (Shell's EPON 825)	2	350
		
Ethylenediamine (EDA)	4	60
		
N-Methylethylenediamine (MEDA)	3	74
		
N,N-Dimethylethylenediamine (DMEDA)	2	88
		

where f is the functionality of the amine, M_f is the molecular weight of f^{th} functional amine; M_e is the epoxide equivalent weight (grams of resin per mole of epoxide) and Φ_f is the mole fraction of amine hydrogens provided by the f^{th} functional amine. Full details on the method used to calculate M_e can be found in the paper by Crawford and Lesser [16].

The DGEBA was conditioned in a vacuum oven at 100 °C and a pressure of 100 kPa for a day, to remove water and air. The resin was cooled to 50 °C and mixed with room temperature curing agents. Before pouring the samples, the mixture was evacuated to remove air bubbles. All samples were cured at 50 °C for 24 h, post cured at 20 °C above the fully cured T_g for 2 h and then slow cooled in the oven. The glass transition temperatures were determined using a differential scanning calorimeter (DSC) with a ramp rate of 10 °C min⁻¹.

2.2. Sample fabrication

ASTM D638 Type I tensile bars [18] were machined from 3.3 mm thick plaques using a specially designed router and die. The samples were then stored in a desiccator for at least 2 days prior to testing.

All multiaxial tests were conducted on thin walled hollow cylinders as shown in Fig. 1. Fabrication of these specimen required a two step process. The first step involves spin casting the hollow tube. A premeasured amount of epoxy is poured into a stainless steel mould, which is then mounted into a specially designed lathe. While spinning, radiant heat is applied to gel the epoxy. The epoxy tube is removed from the mould, the thickness is measured and the ends are corked. In the second step, the end caps are moulded onto the hollow cylinder,

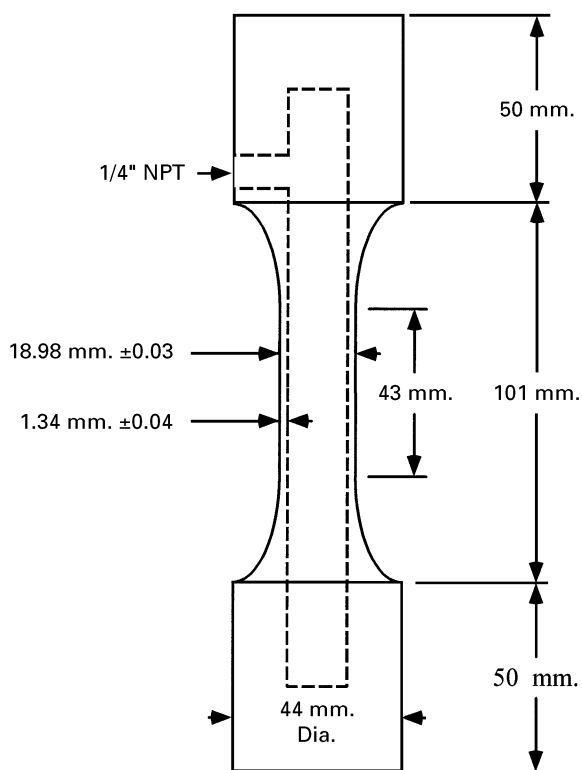


Figure 1 Thin walled hollow cylinder specimen geometry for biaxial tests.

using a mould with a “dumb-bell” configuration. Before the final post cure, the hollow cylinder specimen is removed from the mould and a pressure port is tapped. Finally the sample is stored in a desiccator.

2.3. Testing procedure

All tensile tests were conducted in accordance with the ASTM D638 standard at strain rates specified later in the text. The axial strain rate was controlled by cross-head speed, while both axial and transverse extensometers were attached to the sample to measure the strains. The testing temperature was maintained in an environmental chamber and samples were conditioned for 30 min prior to testing.

The hollow cylinders were tested in an Instron 1321 biaxial tension–torsion machine modified with a Tescom ER3000 digitally controlled pressure regulator, Fig. 2. The samples were pressurized with either nitrogen gas or silicon oil, with no measurable difference found in the yield or fracture strength. Both the tension–torsion machine and the pressure regulator were externally controlled through a personal computer using a program written in LabVIEW.

The hollow cylinders were tested in stress states varying from uniaxial compression to biaxial tension. The LabVIEW test control program maintained a prespecified state of stress, while monotonically

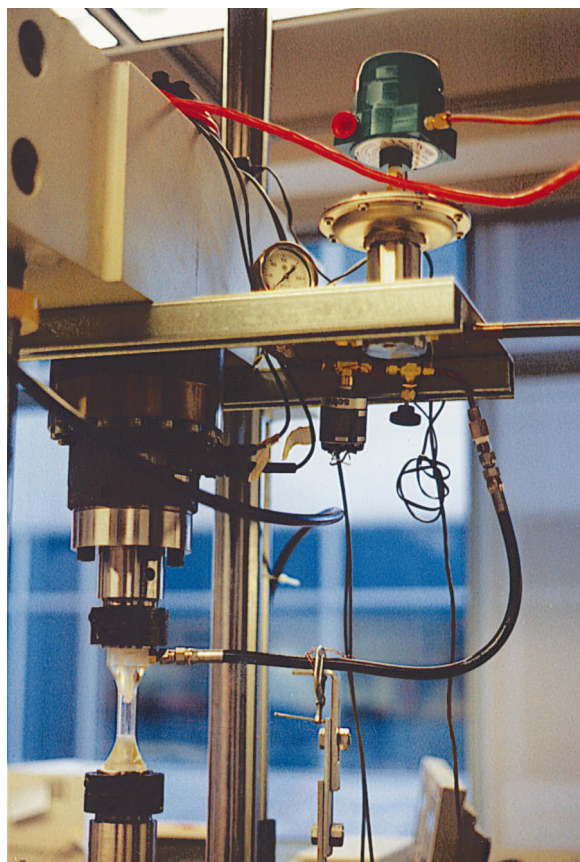


Figure 2 Biaxial testing apparatus. The hollow cylinder specimen is mounted in the biaxial testing machine, while pressure is applied to the sample from the computer controlled pressure regulator at the top of the photograph.

loading the tubes to failure. All tests were conducted at a constant octahedral shear strain rate, $\dot{\gamma}^{\text{oct}}$, for a given failure envelope. Details of this procedure are outlined in the following paragraphs.

The axial and hoop stresses imposed on a thin walled hollow cylinder, subjected to an axial load, L , and internal pressure, p , can be written as:

$$\sigma_a = \left(\frac{L}{\pi D t} + \frac{p D}{4 t} \right) \quad (3)$$

$$\sigma_h = \left(\frac{p D}{2 t} \right) \quad (4)$$

where D is the mean diameter and t is the thickness of the tube. In the absence of an applied torsion, σ_a and σ_h are the principle stresses. The octahedral shear stress, τ^{oct} , and hydrostatic stress, σ_m , can be written as follows:

$$\tau^{\text{oct}} = \frac{1}{3} ((\sigma_a - \sigma_h)^2 + (\sigma_a)^2 + (\sigma_h)^2)^{1/2} \quad (5)$$

$$\sigma_m = \frac{1}{3} (\sigma_a + \sigma_h) \quad (6)$$

The corresponding principle strains were calculated using Equations 7–9.

$$\varepsilon_a = \frac{1}{E} (\sigma_a - \nu \sigma_h) \quad (7)$$

$$\varepsilon_h = \frac{1}{E} (\sigma_h - \nu \sigma_a) \quad (8)$$

$$\varepsilon_r = \frac{-\nu}{E} (\sigma_a - \sigma_h) \quad (9)$$

where ε_a , ε_h and ε_r are the strains in the axial, hoop and radial directions, E is the tensile modulus, and ν is Poisson's ratio.

Preliminary tests were conducted on test specimens with extensometers attached to measure ε_a and ε_h . These tests were used in conjunction with Equations 7–8 to measure and verify the elastic properties. The value of ε_r was not measured in this study and instead it was calculated using Equation 9. For the final tests, in which specimens were tested to failure, the extensometers were removed and Equations 7–9 were used to calculate the strains.

Consistent with linear viscoelastic behaviour, we chose to keep $\dot{\gamma}^{\text{oct}}$ constant during testing. $\dot{\gamma}^{\text{oct}}$ can be written as:

$$\dot{\gamma}^{\text{oct}} = \frac{1}{3} \left(\left(1 - \frac{\varepsilon_h}{\varepsilon_a} \right)^2 + \left(\frac{\varepsilon_h}{\varepsilon_a} - \frac{\varepsilon_r}{\varepsilon_a} \right)^2 + \left(1 - \frac{\varepsilon_r}{\varepsilon_a} \right)^2 \right)^{1/2} \dot{\varepsilon}_a \quad (10)$$

where $\dot{\varepsilon}_a$ is the axial strain rate. $\dot{\varepsilon}_a$ was measured using both an axial extensometer and calculated from the applied stressing rates as follows:

$$\dot{\varepsilon}_a = \frac{1}{E} (\dot{\sigma}_a - \nu \dot{\sigma}_h) \quad (11)$$

where $\dot{\sigma}_a$ and $\dot{\sigma}_h$ are the stressing rates in the axial and hoop directions. As in the case of the tensile tests, the axial strain rate was controlled by the crosshead speed. Note that when testing to failure, $\dot{\gamma}^{\text{oct}}$ is calculated using Equations 7–11. Therefore $\dot{\gamma}^{\text{oct}}$ is held constant only at the desired rate in the linear elastic regime.

3. Results and discussion

3.1. Tensile test results

The tensile tests show how temperature, M_c and strain rate affect E , mode of failure, and the yield or fracture strength in uniaxial tension. Fig. 3 shows how E is effected by temperature and M_c . At 21 °C and $\dot{\gamma}^{\text{oct}} = 0.028 \text{ min}^{-1}$, all the resin systems had approximately the same value of $E \cong 2.6 \text{ GPa}$. The relation between modulus and temperature is similar to that of most thermosets. Similar to the results of others [14, 15], Fig. 3 also shows that below T_g , E is relatively unaffected by changes in M_c . Results from dynamic mechanical thermal analysis (DMTA) also support this, Fig. 4. This is expected since the glassy modulus is controlled by the local chain packing and chain stiffness and not by higher length scale parameters, such as M_c . Figs. 3 and 4 also demonstrate that we have successfully changed M_c without significantly altering the chain stiffness or local packing.

Fig. 5 shows the tensile strength as a function of ΔT , the difference between the testing temperature, T , and T_g at $\dot{\gamma}^{\text{oct}} = 0.028 \text{ min}^{-1}$.

$$\Delta T = (T - T_g) \quad (12)$$

The samples with the three highest M_c values all yielded with their yield strengths decreasing with increased temperature. When the yield strengths of the materials with different M_c values are compared at the same temperature shift below T_g , i.e., constant ΔT , they collapse to a single curve. This ΔT dependence has been previously shown by Bradley *et al.* [19] and suggests that with regard to yield strength, the primary effect of changing M_c is a shift in T_g [20]. There is a possible exception with regard to the materials with $M_c = 380$ and 480 g mol^{-1} . The samples with $M_c = 480 \text{ g mol}^{-1}$ fail in a brittle fashion in uniaxial tension at the lower temperatures, but change their mode of failure from brittle fracture to ductile yield at

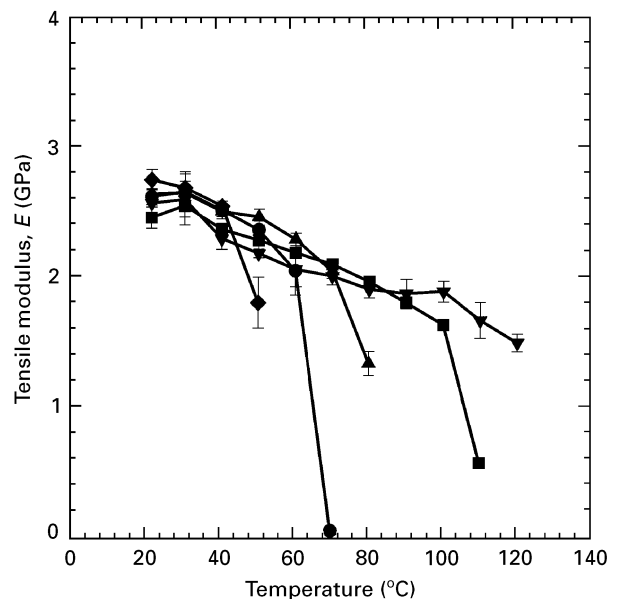


Figure 3 Tensile modulus versus temperature, for DGEBA cured with EDA and MEDA/DMEDA $\dot{\gamma}^{\text{oct}} = 0.028 \text{ min}^{-1}$. Key: M_c values are; (◆) 1790 g mol^{-1} , (●) 950 g mol^{-1} , (▲) 640 g mol^{-1} , (■) 400 g mol^{-1} and (▼) 380 g mol^{-1} .

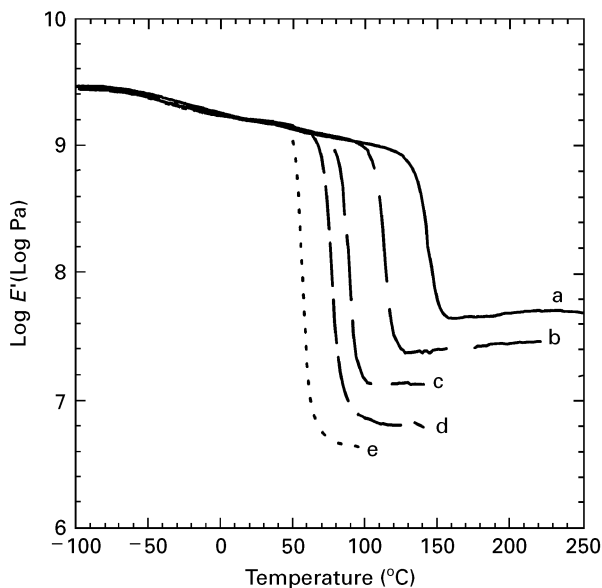


Figure 4 Flexural storage modulus versus temperature at 1 Hz using single cantilever beam DMTA. DGEBA cured with EDA and MEDA/DMEDA. Key: M_c values of; (a) 380 g mol^{-1} , (b) 480 g mol^{-1} , (c) 640 g mol^{-1} , (d) 950 g mol^{-1} and (e) 1790 g mol^{-1} .

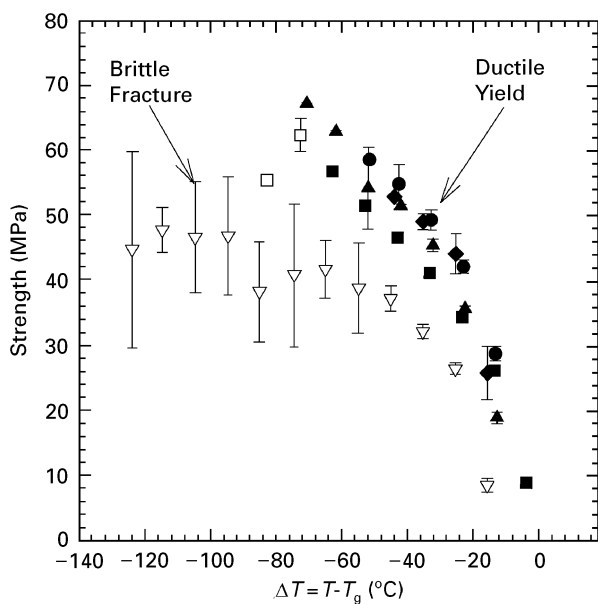


Figure 5 ASTM D638 tensile strength versus ΔT , for DGEBA cured with EDA and MEDA/DMEDA. $\dot{\gamma}^{\text{oct}} = 0.028 \text{ min}^{-1}$. Solid and hollow symbols represent ductile yield and brittle fracture, respectively. Key: M_c values are; (◆) 1790 g mol^{-1} , (●) 950 g mol^{-1} , (▲) 640 g mol^{-1} , (■) 480 g mol^{-1} and (▽) 380 g mol^{-1} .

approximately 40°C . Even at these higher temperatures, the yield strengths of the material with $M_c = 480 \text{ g mol}^{-1}$ do not fully collapse to the curve with the lower M_c materials. As for the samples with $M_c = 380 \text{ g mol}^{-1}$, brittle fracture is the failure mode regardless of temperature. This is a consequence of a network so tightly crosslinked that the yield response is suppressed and brittle fracture is preferred in this stress state.

Fig. 6 shows the effect of strain rate and temperature on tensile yield strength for a typical glassy polymer. The yield strength, σ_y , has been normalized by absolute temperature in accordance with an Eyring

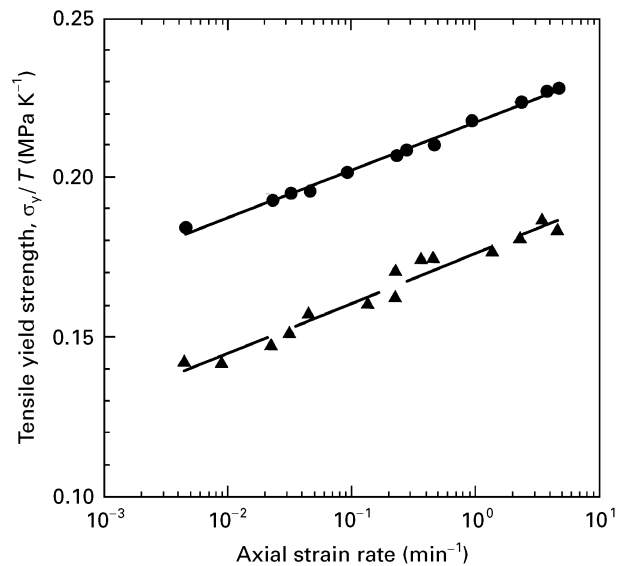


Figure 6 Tensile yield strength versus axial strain rate, for DGEBA cured with EDA and MEDA/DMEDA with $M_c = 950 \text{ g mol}^{-1}$ at (●) 21°C and (▲) 40°C . The slope of the data set at 21°C is $1.57 \times 10^{-2} \text{ (MPa min K}^{-1}\text{)}$.

type equation [21]:

$$\frac{\sigma_y}{T} = \frac{\Delta E}{T v^*} + \frac{R}{v^*} \ln\left(\frac{\dot{\epsilon}}{\Gamma}\right) \quad (13)$$

where ΔE is the activation energy, v^* is the activation volume, $\dot{\epsilon}$ is the strain rate, and Γ is a proportionality constant. The rate dependent tensile yield behaviour of these materials fits an Eyring type flow model quite well. The activation energy of the material with $M_c = 950 \text{ g mol}^{-1}$ was found to be $\Delta E = 247 \text{ kJ mol}^{-1}$.

3.2. Hollow cylinder test results

Quite often, it is useful to compare the stress-strain response when evaluating test results. Similarly, when testing polymeric materials in multiaxial stress states, it is useful to study how volumetric strains affect the mode of failure and the yield or fracture strength of the material. Therefore a plot of τ^{oct} versus engineering volumetric strain, ϵ_m ,

$$\epsilon_m = \frac{1}{3}(\epsilon_a + \epsilon_h + \epsilon_r) \quad (14)$$

provides a qualitative understanding of the loading path under which these tests are run and clearly shows where the ductile-to-brittle transition occurs. Fig. 7 illustrates this for the case of $M_c = 380 \text{ g mol}^{-1}$. Note that from this plot, the ductile-to-brittle transition occurs midway between uniaxial compression and pure shear.

A convenient way to present the yield and fracture response in constrained stress states is to plot the shear yield stress that occurs on the octahedral plane, τ_y^{oct} , as a function of the hydrostatic stress, σ_m , that occurs in that stress state. If the material follows a modified von Mises type behaviour, then the data will plot on a straight line (see Equation 1). If σ_m has no effect on τ_y^{oct} , then the data will plot on a horizontal line and the data is said to follow a typical von Mises behaviour. If however σ_m does influence τ_y^{oct} , then the

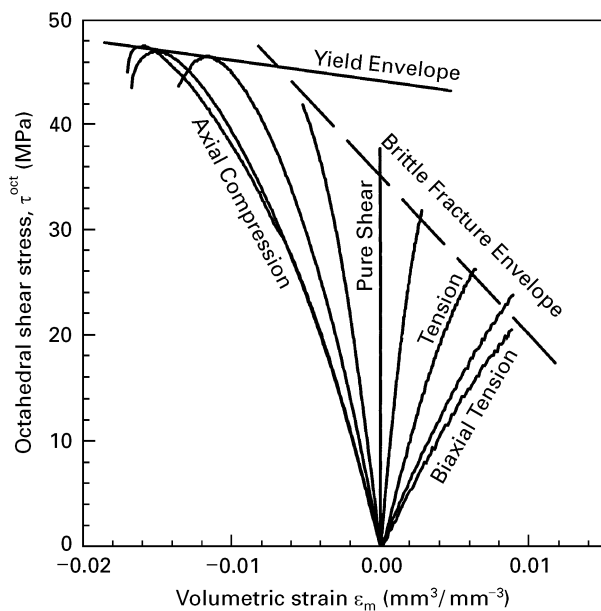


Figure 7 Octahedral shear stress versus volumetric strain on hollow cylinders, illustrating a ductile-to-brittle transition for DGEBA cured with EDA and MEDA/DMEDA with $M_c = 380 \text{ g mol}^{-1}$.

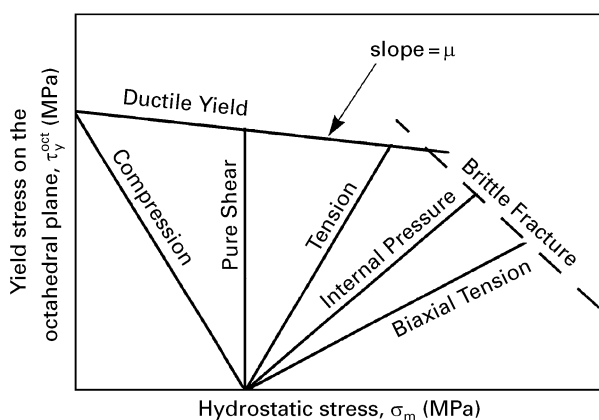


Figure 8 Schematic of typical results obtained for biaxial tests on hollow cylinders, exhibiting a ductile-to-brittle transition.

line will be sloped. The slope of the line, μ , is commonly referred to as the coefficient of internal friction. This is illustrated in Fig. 8.

Following the above scheme, typical results from our hollow cylinder tests are shown in Fig. 9. Also in Fig. 9, we have plotted the results of Sultan and McGarry from the hollow cylinder testing of a DGEBA (Shell EPON 828) cured with Shell Corporation's curing agent D [2]. Both sets of results show that the yield behaviour of epoxy networks follows a modified von Mises criterion. However, Sultan and McGarry reported a value of $\mu = 0.175$, which differs from our reported value of $\mu = 0.157$ for $M_c = 640 \text{ g mol}^{-1}$. Nonetheless, Fig. 9 shows that the data of Sultan and McGarry agrees quite well with our results. We attribute differences in the reported values of μ to the scatter introduced into the data of Sultan and McGarry [2] by higher hydrostatic stress levels, which reflects the difficulty of running accurate experiments in this regime.

Fig. 10 shows the effects that changes in M_c have on the generalized yield and fracture strengths of these

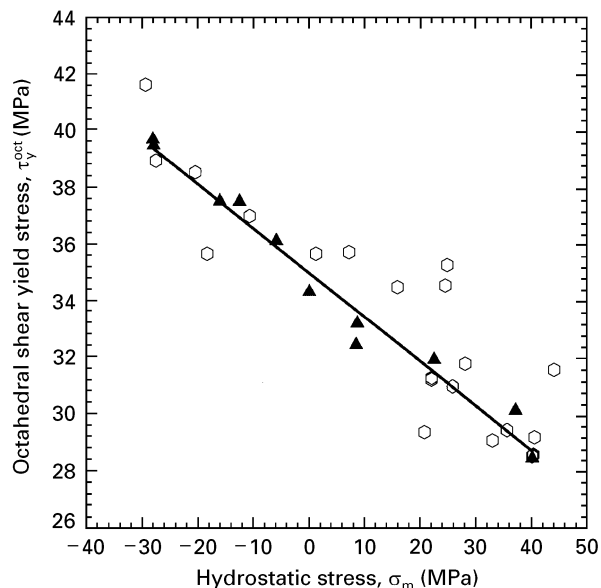


Figure 9 Hollow cylinder octahedral shear yield stress versus hydrostatic stress, for DGEBA cured with EDA and MEDA/DMEDA for (\blacktriangle) $M_c = 640 \text{ g mol}^{-1}$ and $\dot{\gamma}^{oct} = 0.028 \text{ min}^{-1}$; and (\circ) data from Sultan and McGarry [2].

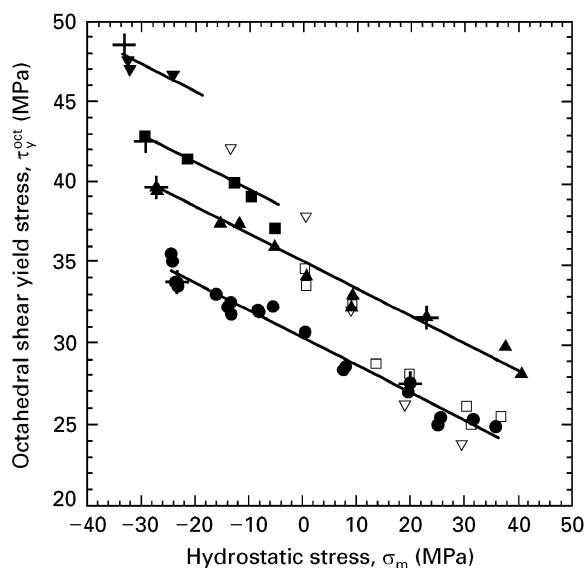


Figure 10 Octahedral shear yield stress versus hydrostatic stress, for hollow cylinders made of DGEBA cured with EDA and MEDA/DMEDA and tested at $\dot{\gamma}^{oct} = 0.028 \text{ min}^{-1}$. The solid symbols and hollow symbols represent ductile yield, brittle fracture, and (+) are the ASTM standard compression and tensile yield results, respectively. Key: M_c values of; (\bullet) 950 g mol^{-1} , (\blacktriangle) 640 g mol^{-1} , (\blacksquare) 480 g mol^{-1} and (\blacktriangledown) 380 g mol^{-1} .

materials. Ductile yield and brittle fracture are represented by solid and hollow symbols, respectively. Note that the yield behaviour follows a modified von Mises criterion for all M_c tested. Further, these results show that changing M_c has the effect of solely changing τ_{y0}^{oct} , while μ is independent of M_c . For reference, yield results from uniaxial compression and tensile bars have also been plotted in Fig. 10. For all M_c , the standard tensile and compressive yield strengths are very close to the hollow cylinder results.

Fig. 10 also shows that as M_c decreases, a ductile-to-brittle transition appears. As shown previously in Fig. 7, for $M_c = 380 \text{ g mol}^{-1}$ this ductile-to-brittle

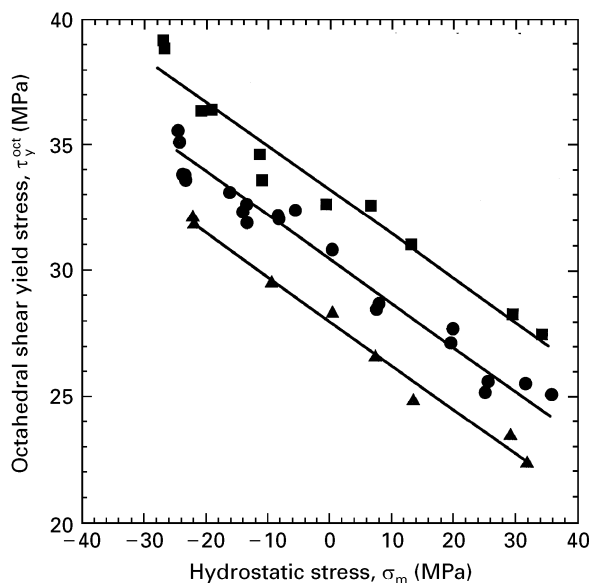


Figure 11 Octahedral shear yield stress versus hydrostatic stress, for hollow cylinders made of DGEBA cured with EDA and MEDA/DMEDA with $M_c = 950 \text{ g mol}^{-1}$, tested at strain rates of (\blacktriangle) 0.0028 min^{-1} , (\bullet) 0.028 min^{-1} and (\blacksquare) 0.28 min^{-1} .

transition occurs midway between uniaxial compression and pure shear. Although further testing is needed to elucidate the effects that changing M_c has on brittle fracture, two statements can be made. First, the fracture strength of these materials is more significantly influenced by σ_m than is the corresponding yield strength. And second, this influence is also sensitive to changes in M_c .

In addition to changing M_c , the strain rate was also varied. Fig. 11 shows that for $M_c = 950 \text{ g mol}^{-1}$, tested at 21°C and $\dot{\gamma}^{\text{oct}} = 0.0028, 0.028$ and 0.28 min^{-1} , only τ_{y0}^{oct} is affected by a change in the strain rate. In contrast μ remains insensitive to changes in $\dot{\gamma}^{\text{oct}}$, with $\mu = 0.172, 0.163$, and 0.173 for $\dot{\gamma}^{\text{oct}} = 0.0028, 0.028$ and 0.28 min^{-1} , respectively. This is in contrast to the general statement made by Kinloch [6], regarding the effects of strain rate on μ . However tests by Duckett *et al.* have also shown μ to be insensitive to strain rate [4]. Furthermore, the $\dot{\gamma}^{\text{oct}}$ induced increase in τ_{y0}^{oct} can be directly compared with our tensile data for the same material (see Fig. 6). The hollow cylinders showed a strain rate dependence on τ_{y0}^{oct} of 2.6 MPa per decade increase in strain rate, which is close to the 2.2 MPa per decade obtained for the tensile tests at 21°C .

4. Conclusions

We conducted this study to more fundamentally investigate the yield and fracture response of glassy polymers subjected to constrained stress states. Our tests have elucidated the effects that stress state, M_c , strain rate and testing temperature have on the yield and fracture response of these materials.

Our first set of experiments showed that the yield response of glassy epoxy networks phenomenologically follows a modified von Mises yield criterion over the range of stress states, strain rates, and M_c tested. Furthermore, changes in $\dot{\gamma}^{\text{oct}}$, only affect τ_{y0}^{oct} as

described by an Eyring type flow process (Equation 13). The coefficient of internal friction, μ , is insensitive to changes in strain rate over the range tested. Finally, it was found that changes in M_c also affect τ_{y0}^{oct} only, and μ again remains constant over the range of M_c tested.

Although further studies are needed to fully understand the effects of M_c and test conditions on the brittle fracture and the brittle-to-ductile transition in epoxy networks, it is clear that the effects can be significant. At this point it is not clear how the brittle-to-ductile transition is affected by M_c . However, there is strong evidence that the pressure dependence on fracture is sensitive to M_c .

Acknowledgements

The authors gratefully acknowledge the Materials Research Science and Engineering Centre (MRSEC) and the Shell Foundation for support of this study. We are also grateful for the thoughtful discussions with Piero Puccini and Steve Corley of Shell Development Company.

References

1. S. S. STERNSTEIN and L. ONGCHIN, *A.C.S. Polym. Prep.* **10** (1969) 1117.
2. J. N. SULTAN and F. J. MCGARRY, *Polym. Engng. Sci.* **13** (1973) 29.
3. L. M. CARAPPELLUCCI and A. F. YEE, *ibid.* **26** (1986) 920.
4. R. A. DUCKETT, C. BINODE, L. GOSWAMI, S. SMITH, I. M. WARD and A. M. ZIHLIF, *Brit. Polym. J.* **10** (1978) 11.
5. I. M. WARD, *J. Mater. Sci.* **6** (1971) 1397.
6. A. J. KINLOCK, "Fracture behaviour of polymers" (Applied Science Publishers, London, 1983).
7. R. L. THORKILDSEN, in "Engineering design for plastics", edited by E. Baer (Reinhold, New York, 1964) p. 277.
8. P. B. BOWDEN and J. A. JUKES, *J. Mater. Sci.* **3** (1968) 183.
9. R. RAGHAVA, R. W. CADDELL and G. H. YEH, *ibid.* **8** (1973) 225.
10. W. WHITNEY and R. D. ANDREWS, *J. Polym. Sci. C* **16** (1967) 2891.
11. A. S. ARGON, R. D. ANDREWS, J. A. GODRICK, W. WHITNEY, *J. Appl. Phys.* **39** (1968) 1899.
12. S. S. STERNSTEIN, L. ONGCHIN and A. SILVERMAN, *Appl. Polym. Symp.* **7** (1968) 175.
13. R. A. DUCKETT, S. RABINOMITS, I. M. WARD, *J. Mater. Sci.* **5** (1970) 909.
14. J. M. CHARLESWORTH, *Polym. Engng. Sci.* **28** (1988) 230.
15. L. E. NIELSEN, *J. Macromol. Sci.-Revs. Macromol. Chem.* **C3** (1969) 69.
16. E. D. CRAWFORD and A. J. LESSER, *J. Appl. Polym. Sci.* (accepted May, 1997).
17. A. J. LESSER and R. S. KODY, *J. Polym. Sci.: Part B: Polym. Phys.* (accepted January, 1997).
18. "1987 Annual book of ASTM standards", V08.01 (American Society for Testing and Materials, Philadelphia, PA, 1987) D638-86.
19. W. L. BRADLEY, W. SCHULTZ, C. CORLETO, A. S. KOMATSU, "Toughened plastics I" (American Chemical Society, Washington, D.C., 1993) p. 233.
20. B. L. BURTON and J. L. BERTRAM, "Polymer toughening" (Marcel Dekker, New York, 1996).
21. H. EYRING, *J. Chem. Phys.* **4** (1936) 283.

Received 17 October 1996
and accepted 22 May 1997